EFFECTS OF VARIABLE PRESSURE GRADIENT ON MAGNETOHYDRODYNAMIC FLOW BETWEEN PARALLEL PLATES CONSIDERING VARIABLE TRANSVERSE MAGNETIC FIELDS

BY

KIMANTHI PRISCILLA TWILI B.Ed. (science)

REG NO: I56/CE/25461/2018

MATHEMATICS AND ACTUARIAL SCIENCES DEPARTMENT

A Research Project Submitted in Partial Fulfillment of the Requirements for the Award of the Degree of Masters of Science in Applied Mathematics in the School of Pure and Applied Sciences of Kenyatta University.

NOVEMBER 2022.

DECLARATION

This research project is my original work and has not been presented for a degree in any other university or award.

Priscilla Twili Kimanthi

Signature……. Date……

Department of Mathematics and actuarial sciences

I confirm that the above candidate did the work reported in this research project under my supervision.

Dr. Isaac Chepkwony

Signature……. Date……

Department of Mathematics and actuarial sciences

School of pure and applied sciences

Kenyatta University

DEDICATION

To my parents, John Kimanthi and Josephine Kakina, I extend my warmest gratitude for your love, encouragement, and support during my master's course. I pen a unique feeling of dedication and appreciation to my twin sister, Esther Mbatha, for her love and friendship. May this work challenge and motivate you to commence your master's program.

ACKNOWLEDGEMENTS

I gratefully acknowledge and appreciate the contribution of Dr. Isaac Chepkwony, Kenyatta University. Through his counsel, advice, timely reading, and corrections of this study, I could sail through with fewer difficulties. His support and enlightenment kept me on track throughout the study.

I also extend my gratitude to my course mates Ethel, John, and Simon, who walked and worked together as a team during coursework studies. My special thanks to Simon for his help during the MATLAB analysis.

ABSTRACT

Analysis of the effects of applying a variable pressure gradient to a magnetohydrodynamic fluid flowing between two parallel plates under the influence of variable transverse magnetic fields was investigated. The study involved a steady, incompressible hydromagnetic fluid flowing through parallel plates. The upper plate was considered porous, moving opposite the fluid flow, while the lower plate remained immovable. The equations governing the flow include the conservation of mass, energy, Navier-Stokes, and electromagnetic equations. The equations were made dimensionless and then solved using the Finite Difference Method. Matrix laboratory (R2018b) was used to solve and analyze the finalized equations for velocity and temperature profiles for various thermo-physical parameters. The final results were illustrated graphically and discussed quantitatively. The results indicated that Reynold's number is inversely proportional to velocity distribution and temperature profile. The increasing magnetic parameter led to increased fluid temperature and decreased velocity profile. Eckert number and Prandtl parameter did not affect velocity profiles. Also, increasing the suction parameter yielded decreased velocity and increased temperature profile. When the pressure gradient was increased, velocity decreased as temperature increased. The temperature of the fluid increased when the Eckert number was increased and decreased as the Prandtl parameter increased. An increase in Hartmann's number yielded a higher temperature profile. The results obtained in this research provide valuable information to different fields, especially in designing and modeling systems in dyeing industries, cooling of automobile moving parts, and extraction of metal industries. Moreover, the findings apply to Magnetodydrodynamic flow through a porous medium, widely used in magnetohydrodynamic power generators, aerodynamic heating, and separation of matter from liquids mixed using a centrifugal separator.

ACRONYMS AND ABBREVIATIONS

SYMBOLS	MEANING
a	Distance between the parallel sheets
$\vec{B}$	Magnetic flux density
C_P	Heat capacity of the fluid
E_C	Eckert parameter number
$\vec{E}$	Electric field strength
e	Specific internal energy constant
Fx, Fy, Fz	Body forces
G	Volumetric constant
H_a	Hartmann parameter
$\vec{H}$	Magnetic field strength
$\vec{J}$	Electrical current density
K	Thermal conductivity
L	Characteristic Length
M	Magnetic number
P_r	Prandtl parameter
P^*	Dimensionless Pressure
P	The pressure of the fluid
q_j	Quantity of heat
Re	Reynold's parameter
r	Specific enthalpy
$S_\circ$	Suction parameter
s	Entropy

T_W	The characteristic temperature on the sheets
T	The temperature of the fluid
T_∞	Characteristic temperature
t^*	Dimensionless time
t	Time
u, v, w	Velocity components in the Cartesian axis
U^* , V^*	Dimensionless velocity components
U	Characteristic velocity
$\vec{V}$	Velocity
x, y, z	Cartesian coordinates
X^* , Y^*	Dimensionless Cartesian coordinates
$\frac{\partial P}{\partial x}$	Pressure gradient
Δt	Change in time
φ	Dissipation function
μ	Viscosity Coefficient
μ_e	Magnetic permeability
σ	Electrical conductivity
∇	Gradient operator
ρ	Density
Δy	Change in distance
∇^2	Laplacian operator

ABBREVIATIONS

FDM	Finite Difference Method
MHD	MagnetoHydroDynamics
PDE	Partial Difference Equation
MATLAB	Matrix Laboratory

TABLE OF CONTENTS

LIST OF FIGURES

CHAPTER ONE

BACKGROUND INFORMATION AND INTRODUCTION

Liquids and gases are commonly referred to as fluids. Fluid can be defined as any material that experiences a continuous change in shape and state when subjected to shear stress. Fluids are categorized as Newtonian and non-Newtonian fluids. In Non-Newtonian fluids, viscosity changes with varying shear rates, while Newtonian fluids have constant viscosity as shear force varies. Viscosity can be described as the relationship between velocity slope and shear force. However, kinematic viscosity relates the mass per unit volume of a fluid to its viscosity. Viscosity determines the force that must be overcome when fluids are used in lubrication, smoothening, and pipeline transportation. It regulates fluid flow in injection molding, surface coating, and spraying.

Incompressible fluid between parallel plates normal to them is referred to as Hartmann. Hartmann number (Ha) is the ratio of electromagnetic force to the viscous force experienced by fluid flow through magnetic fields. Viscosity is the degree of fluid opposition to the motion. Viscosity distinguishes ideal from real fluids. Ideal fluids do not offer drag or internal opposition on the wall of channels as it lacks viscosity.

Magnetohydrodynamics analyzes the properties of electrically conducting fluids and the forces that influence them when acted upon by a magnetic field through various channels. Electrically conducting fluids include liquid metals and ionized gases. Under magnetic fields, the flow of an electrically conducting fluid induces electric currents, and therefore Lorentz force, F, described by the formula $J \times B$ is developed. The induced currents successively produce their magnetic fields, consequently influencing the state of the

original magnetic fields. The Lorentz force law describes the force acting on a fluid moving under the influence of magnetic fields and electric fields.

A porous medium is a collection of interconnected solid bodies with pores through which fluid passes. Fluid flowing through permeable material is quantified by Darcy's law which relates discharge per unit area of the cross-section to the pressure gradient of fluid through a porous medium. The critical characteristic of porous media is porosity, n, which is the extent of the fluid capacity of the medium. Flows through permeable membranes apply to many scientific and engineering fields. MHD through porous media has various applications, including underground energy transport and petroleum engineering in analyzing groundwater pollution and purifying crude oil. Porous plates can also cover a heated body to regulate temperature and reduce natural convection.

Fluid flow is described as unsteady or steady. Fluids' properties like density, pressure, and velocity applied to magnetic field and temperature do not depend on time and are referred to as steady fluids. In unsteady flow, pressure, density, and velocity properties are time-dependent.

STATEMENT OF THE PROBLEM

Magnetohydrodynamic flow through a porous medium is widely utilized in cooling automobiles, centrifugal separation, and aerodynamic heating. Past research has used several techniques to show how the flow is affected by pressure gradient and magnetic fields. However, little focus has been given to the effect of pressure gradient on MHD flow considering a porous medium where the magnetic field is at right angles to the fluid flow. Our research analysis aims to investigate the outcomes of; the Eckert number, Pressure gradient, Hartmann number, Prandtl number, Reynolds number, Suction parameter, and Magnetic number and their consequence on velocity and temperature profiles due to a variable pressure gradient on MHD fluid flow between parallel plates. Variable transverse magnetic fields act on the porous upper plate. The fluid is considered to be steady, incompressible, and viscous. When the fluid is at rest, at $t = 0$, both plates are stationary, and at t greater than zero $(t > 0)$, the lower plate is immobile as the top plate move in the opposite direction to the fluid flow. The two plates are considered to be of infinite length in the $x -$ and $z -$ directions, and transverse magnetic fields act on the $y -$ axis. The plates are at a distance '$2a$' apart.

JUSTIFICATION

Past research investigations studied uniform pressure gradients applied to equidistant plates and varying perpendicular magnetic fields. In this research study, variable pressure gradient, which generalizes uniform pressure gradients, is applied to parallel plates with variable transverse magnetic fields. The results obtained in this research provide valuable information to different fields, especially in designing and modeling systems in dyeing industries, cooling of automobile moving parts, and extraction of metal industries.

Moreover, the findings apply to Magnetodydrodynamic flow through a porous medium, widely used in magnetohydrodynamic power generators, aerodynamic heating, and separation of matter from liquids mixed using a centrifugal separator.

OBJECTIVES

i. General objectives

To determine the consequence of applying variable pressure gradient on various thermo-physical parameters considering a Magnetohydrodynamic fluid flow constrained in two parallel plates with varying magnetic fields at right angles.

ii. Specific objectives

i. To determine temperature distributions of the fluid stream bounded by the parallel plates.

ii. To determine the velocity profile of the fluid stream bounded by parallel plates.

iii. To determine the outcome of differing suction parameters, Eckert number, pressure gradient magnetic parameter, Prandtl parameter, Hartmann parameter, and Reynolds number on temperature profile and velocity distribution.

Significance of the study

MHD flow between parallel porous channels has various uses in MHD power generators, aerodynamic heating and separation of solids from fluids, purifying crude oil, sprays, cooling systems, polymer technology, and the petroleum industry. Transpiration cooling is essential in minimizing heat transmission on a body's boundary layer with many applications, including moving parts of automobile machines, rockets, and jets and chilling atomic reactors.

CHAPTER TWO

LITERATURE REVIEW

Magnetohydrodynamic fluid flow has been researched in the past. This chapter emphasizes research investigations related to the research topic and their findings.

Shercliff (1953) considered an electrically conducting fluid that was steady and viscous through a channel where transverse magnetic fields were applied, and the boundaries were insulators. He developed a solution for channels of all well-proportioned shapes. He observed pressure gradients for given flow volumes at various strengths, which compared well with the experimental results for circular and square shapes.

Non-Newtonian incompressible fluid in an unbending tube and round section exposed to a periodic pressure gradient was studied by Jones and Walters (1967). Although the nature of the flow was identical to a purely viscous fluid, they also deduced that elasticity could affect the magnitude and location of the top mean velocity.

The hydromagnetic flow of a conducting liquid through an infinite permeable flat material with the Hall Effect was investigated by Gupta (1975). The infinite porous plates experienced transverse magnetic fields. He concluded that there was an exact solution for suction or blow at the plates for the magnetic field. Also, a small Reynolds number obtained a flow relatively near to a non-conducting fluid through a membrane in a circulating flame.

Hassanien (1991) analyzed an electrically conducting fluid past a porous material enclosed by infinite sheets. The lower plate was fixed while the top plate was rotating on its axis, acted upon by perpendicular magnetic fields. The fluid was considered unsteady,

viscous, and incompressible in two dimensions. They concluded that axial velocity increase with increasing entrance velocity and reduces on reducing Hartmann's number.

Jat and Jhankal (2003) studied three-dimensional free convection magnetohydrodynamic flows with heat transfer of viscoelastic incompressible fluid enclosed by an endless permeable plate flowing in a porous media. They found a significant impact on heat transfer and magnetic field permeability. Investigations on Magnetohydrodynamic stokes flow were done by Ganesh and Krishnambal (2007). The fluid was considered unsteady and viscous, flowing through a channel with magnetic fields at right angles. They deduced that the greater the Hartmann number, the lower the magnitude of the axial velocity profiles.

Rajput and Sahu (2011) analyzed a uniform transverse magnetic field of electrically conducting convection flow unsteady, incompressible, and viscous. Manyonge *et al.* (2012) investigated the two-dimensional magnetohydrodynamic poiseuille flow of incompressible steady fluid. The fluid flowed between porous channels influenced by a slanting magnetic field and uniform pressure gradient. The analysis obtained showed that velocity distribution decreased as magnetic field strength increased.

Unsteady Magnetohydrodynamic Couette flow between infinite porous plates where the lower plate was considered porous past a sloped magnetic field with heat transmission was analyzed by Joseph *et al.* (2014). They found out that a high magnetic field reduced energy losses. Singh (2014) studied the steady laminar flow of viscous incompressible fluid between two parallel infinite plates with a constant pressure gradient. The results showed that increasing the magnetic field's inclination decreased the velocity profile.

Kiema *et al.* (2015) studied MHD fluid steadily flowing with a constant pressure gradient between two limitless parallel pervious sheets under a steady magnetic field. The fluid entered through the lower sheet and exited through the top sheet. The results showed that velocity was lowered whenever the Hartmann number was increased. Unsteady and incompressible MHD fluid within a revolving porous medium, hall current and exposure to varying pressure gradient was discussed by Krishna (2016). It was found that the existence of hall current and pressure gradients on a revolving and Lorentz forces influence velocity distributions.

Mbugua *et al.* (2016) investigated the electrically conducting flow of incompressible unsteady Newtonian fluid flowing through porous non-conducting sheets in the variable transverse magnetic field. The top sheet moved contrary to the fluid flow as the bottom sheet remained stationary. The pressure gradient was taken to be uniform throughout. They concluded that the reduced suction parameter increased the velocity distribution and decreased the temperature profiles. They also deduced that suction stabilized the boundary layer growth. MHD fluid through parallel plates subject to an inclined magnetic field under a uniform pressure gradient was studied by Mburu *et al.* (2016). They found that an increase in Hartmann's number lowered velocity and pressure gradient directly proportional to velocity.

Dash & Ojha (2018) studied viscoelastic hydromagnetic flow between two permeable sheets in the presence of a sinusoidal pressure gradient and a magnetic field and porous matrix. They found out that the flowing back of fluid could be prevented by having pressure gradient oscillation at low frequency. Malia, M. (2018) investigated variable pressure gradients on an unsteady Magnetohydrodynamic fluid flow between two

bounded sheets with inclined magnetic fields. The conclusions showed that increasing Reynold's and suction parameters lowers velocity distributions. Using the finite difference method, the MHD flow of two parallel plates influenced by a sliding magnetic field was analyzed by Aruna and Dubewar (2019). They confirmed earlier that velocity decreased as the slant angle increased.

Kane I. *et al.* (2020) studied two equidistant sheets in motion with unsteady fluid flowing between them under the influence of inclined enforced magnetic fields. They deduced that temperature increases with increasing magnetic parameters, Eckert number, and suction parameters. Moses *et al.* (2021) researched Poiseuille oscillatory flow between limitless equidistant sheets with an inclined magnetic field and suction effect applied. The investigations indicated that greater values Hartmann parameter reduces the velocity of the flow.

Earlier researchers have investigated various MHD flows. Previous research by Malia, M. (2018) investigated the effect of applying variable pressure gradient on Magnetohydrodynamic flow between porous plates and inclined magnetic fields. This study analyzes the effects of variable pressure gradient applied to MHD fluid when the magnetic fields are transverse to the upper plate.

CHAPTER THREE

3.1 OVERVIEW

This section describes the model used and the research problem. The equations governing this MHD fluid flow were reformulated to fit our specific research.

3.2 MATHEMATICAL MODEL

In this research, we analyze a two-dimensional magnetohydrodynamic fluid flowing through equidistant sheets influenced by an adjustable pressure gradient and varying magnetic field acting perpendicular to the porous top plate moving with even suction.

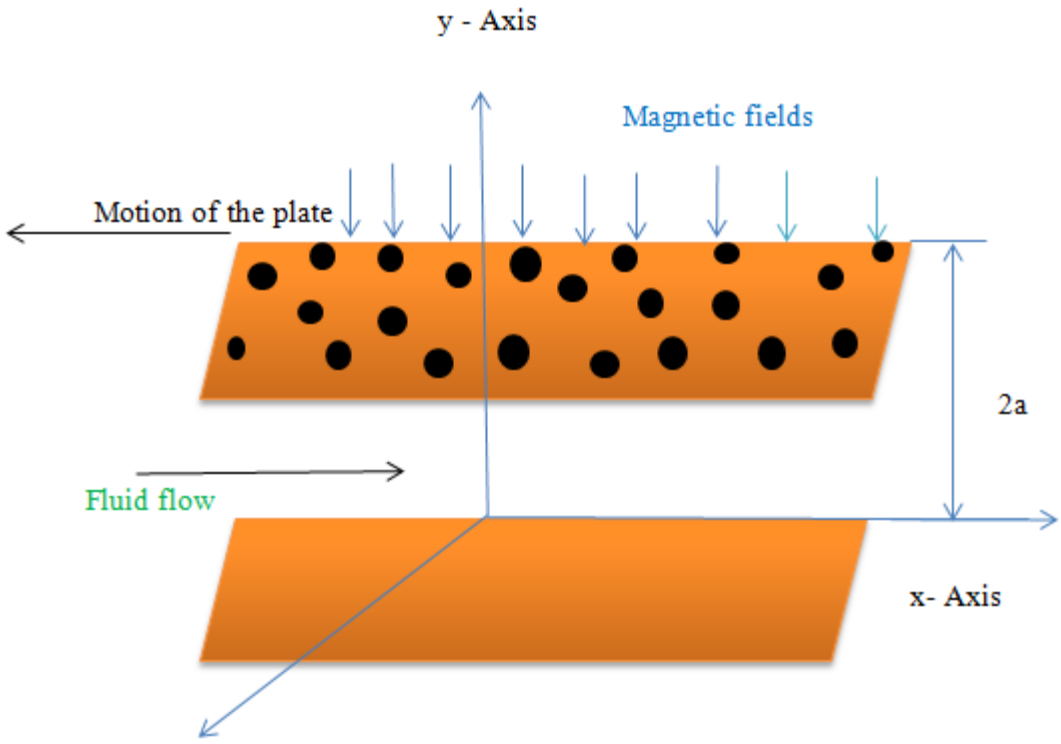

Figure1. Structure of the flow

The plates are placed at a distance of 2a apart. The two plates have an unlimited length in the $z-$ and $x-$ directions. Also, varying transverse magnetic fields are exerted perpendicular to the y-axis of the top sheet. When the fluid is at rest, $t = 0$, both the fluid

and the plates are stationary. When $t > 0$, the upper plate move contrary to the fluid flow as the bottom non-porous plate remains stationary. Fig.1 illustrates this description.

Assumptions made during this study analysis are;

a) The fluid flows in two- dimensions.
b) The fluid remains incompressible and steady.
c) In the x −direction and z −direction, the plates have immeasurable lengths.
d) The viscosity coefficient, electrical conductivity, and thermal conductivity remain constant.
e) The no-slip condition is satisfied.
f) The fluid does not undergo any chemical change.

3.3 GOVERNING EQUATIONS

1. CONTINUITY EQUATION

Mass conservation indicates that one cannot generate or destroy mass. Thus, the degree to which a fluid flows into and out of control volume is equal. In tensor form, the equation of continuity is given by,

$$\frac{\partial \rho}{\partial t} + \frac{\partial}{\partial x_i}(\rho u_i) = 0. \qquad (3.3.1.1)$$

Where $i = 1,2,3$ represent x-, y-, and z- directions, respectively. Since the flow is steady and incompressible, the density of fluid does not change with time, and equation (3.3.1.1) becomes,

$$\frac{\partial}{\partial x_i}(u_i) = 0. \qquad (3.3.1.2)$$

Writing in Cartesian coordinates, equation (3.3.1.2) becomes,

$$\frac{\partial u}{\partial x}+\frac{\partial v}{\partial y}+\frac{\partial w}{\partial z}=0. \quad (3.3.1.3)$$

Since the parallel plates are of immeasurable length in x- and z- directions, the velocity components do not depend on x and z. Consequently, equation (3.3.1.3) becomes

$$\frac{\partial v}{\partial y}=0, \quad (3.3.1.4)$$

Resulting to

$$\partial v=0 \quad (3.3.1.5)$$

$$v=v_{\circ} \quad (3.3.1.6)$$

Where $v_{\circ}$, represent the suction velocity of the porous top plate.

2. ELECTROMAGNETIC EQUATIONS

Electromagnetic equations describe the connection linking the magnetic induction field ($\vec{B}$) of strength $\overrightarrow{H}$, the electric field ($\vec{E}$), electric displacement (D), and current density generated ($\vec{J}$). By Gauss' law of electricity, total electric flux in an enclosed surface increases with an increase in fixed electric charge.

That is,

$$\nabla.\vec{B}=0. \quad (3.3.2.1)$$

Altering magnetic field through a conductor produces an electric current according to Faraday's law of induction.

$$\nabla \times \vec{E} = -\frac{\partial \vec{B}}{\partial t} \quad (3.3.2.2)$$

Where $\vec{B} = \mu_e \overrightarrow{H}.$ (3.3.2.3)

Lorentz's force involves magnetic and electric fields in the presence of electromagnetic fields. Force experienced by an atom of charge q in an electric field $\overrightarrow{E}$ through magnetic induction field $\vec{B}$ and traveling with a velocity $\vec{V}$ is given by

$$\vec{F} = q\vec{E} + q\vec{V} \times \vec{B}. \quad (3.3.2.4)$$

The sum of the momentum of bodies acting on each other in an isolated system remains constant unless external forces act on them, as expressed by the equation of conservation of linear momentum. Considering Ohms law equation,

$$\vec{J} = \sigma\left(\vec{E} + \vec{V} \times \vec{B}\right) \quad (3.3.2.5)$$

But from assumptions, forces due to the electric field are negligible, therefore

$$\vec{J} = \sigma\left(\vec{V} \times \vec{B}\right). \quad (3.3.2.6)$$

Also, the velocity vector of the fluid

$$\vec{V} = \vec{V}(U, 0,0). \quad (3.3.2.7)$$

Then,

$$\vec{V} \times \vec{B} = \vec{J} = \begin{vmatrix} i & j & k \\ U & 0 & 0 \\ 0 & B_y & 0 \end{vmatrix} \sigma = \sigma U B_y k. \quad (3.3.2.8)$$

Applying the Lorentz force equation

$$\vec{J} \times \vec{B} = \begin{vmatrix} i & j & k \\ 0 & 0 & \sigma U B_y \\ 0 & B_y & 0 \end{vmatrix} = -\sigma B_y^2 U i. \quad (3.3.2.9)$$

Substituting magnetic permeability equation $B_y = \mu_e H_y$ to equation (3.3.2.9), we get,

$$\vec{J} \times \vec{B} = -\sigma \mu_e^2 H_y^2 U i. \quad (3.3.2.10)$$

Therefore the Lorentz force experienced was given by,

$$\vec{F} = -U\sigma \mu_e^2 H_y^2. \quad (3.3.2.11)$$

3. NAVIER-STOKES EQUATION

Newton's second law of motion asserts that the momentum variation per unit of time corresponds to the sum of resultant external forces exerted on the body. These external forces include body forces and surface forces. In this research, we considered magnetic force, electric force, and shear stress. The gravitational force was taken to be negligible. The general Navier- Stokes Equation in tensor form is expressed as,

$$\rho \left(\frac{\partial ui}{\partial t}\right) + u_j + \left(\frac{\partial u_i}{\partial x_j}\right) = - \frac{\partial P}{\partial xj} + \mu \nabla^2 ui + \rho F_i \,. \quad (3.3.3.1)$$

Where *i*= 1, 2, 3 and j= 1, 2, 3 vary in the Cartesian plane.

$$\nabla^2 = \frac{\partial^2}{\partial x^2} + \frac{\partial^2}{\partial y^2} + \frac{\partial^2}{\partial z^2} \,. \quad (3.3.3.2)$$

We consider a 2- dimensional flow, and hence,

$$U \frac{\partial u}{\partial x} + V \frac{\partial u}{\partial y} + \frac{\partial u}{\partial t} = \left(\frac{\partial^2 u}{\partial x^2} + \frac{\partial^2 u}{\partial y^2} + \frac{\partial^2 u}{\partial z^2}\right) \frac{\mu}{\rho} - \frac{1}{\rho} \frac{\partial P}{\partial x} + \frac{F_x}{\rho} \quad (3.3.3.3)$$

$$U\frac{\partial v}{\partial x}+V\frac{\partial v}{\partial y}+\frac{\partial v}{\partial t}=\ \left(\frac{\partial^2 v}{\partial x^2}+\frac{\partial^2 v}{\partial y^2}+\frac{\partial^2 v}{\partial z^2}\right)\frac{\mu}{\rho}-\frac{1}{\rho}\frac{\partial P}{\partial y}+\frac{F_y}{\rho} \qquad (3.3.3.4)$$

The velocity profile in the y-axis is zero from the assumptions since the flow is only in x-the direction. Thus equation (3.3.3.3) and (3.3.3.4) respectively becomes,

$$U\frac{\partial u}{\partial x}+V\frac{\partial u}{\partial y}+\frac{\partial u}{\partial t}=\ \left(\frac{\partial^2 u}{\partial x^2}+\frac{\partial^2 u}{\partial y^2}+\frac{\partial^2 u}{\partial z^2}\right)\frac{\mu}{\rho}-\frac{1}{\rho}\frac{\partial P}{\partial x}+\frac{F_x}{\rho} \qquad (3.3.3.5)$$

$$0=\ \frac{F_y}{\rho}-\frac{1}{\rho}\frac{\partial P}{\partial y} \qquad (3.3.3.6)$$

In equation (3.3.3.6), gravitational forces are considered negligible,

$F_y = 0$

Therefore, $-\frac{1}{\rho}\frac{\partial P}{\partial y}=0$

$0=\frac{\partial P}{\partial y}$

$$P = P(x) \qquad (3.3.3.7)$$

The plates are of immeasurable length in x- and z- directions, which simplifies equation (3.3.3.5) to

$$\frac{\partial u}{\partial t}+V\frac{\partial u}{\partial y}=\ -\frac{1}{\rho}\frac{\partial P}{\partial x}+\ \frac{\mu}{\rho}\frac{\partial^2 u}{\partial y^2}+\frac{F_x}{\rho} \qquad (3.3.3.8)$$

Substituting equation (3.3.1.6) to equation (3.3.3.8) we get

$$\frac{\partial u}{\partial t}+v_\circ\frac{\partial u}{\partial y}=\ -\frac{1}{\rho}\frac{\partial P}{\partial x}+\ \frac{\mu}{\rho}\frac{\partial^2 u}{\partial y^2}+\frac{F_x}{\rho} \qquad (3.3.3.9)$$

Body forces are given by Lorentz force described by equation (3.3.2.11) thus,

$$\frac{\partial u}{\partial t} + v_{\circ}\frac{\partial u}{\partial y} = -\frac{1}{\rho}\frac{\partial P}{\partial x} + \frac{\mu}{\rho}\frac{\partial^2 u}{\partial y^2} - \frac{U\sigma\mu_e^2 H_y^2}{\rho} \quad (3.3.3.10)$$

The fluid is considered steady; therefore, equation (3.3.3.10) reduces to

$$v_{\circ}\frac{\partial u}{\partial y} = -\frac{1}{\rho}\frac{\partial P}{\partial x} + \frac{\mu}{\rho}\frac{\partial^2 u}{\partial y^2} - \frac{U\sigma\mu_e^2 H_y^2}{\rho} \quad (3.3.3.11)$$

4. ENERGY EQUATION

Energy can neither be generated nor ruined; however, it can be converted to different forms of energy according to the first law of thermodynamics. The tensor form of this equation is written as

$$\rho\left(\frac{\partial r}{\partial t}\right) + \frac{\partial}{\partial x_j}\left(\rho u_j r\right) = \frac{\partial P}{\partial t} + \frac{\partial}{\partial x_j}\left(u_i P\right) - \frac{\partial q_j}{\partial x_j} + \varphi\,. \quad (3.3.4.1)$$

In x- and z- directions, the plates have an immeasurable length

$$\frac{\partial u}{\partial x} = 0,\ \varphi = \mu\frac{\partial^2 u}{\partial y^2} and\ \ \frac{\partial v}{\partial y} = 0\,. \quad (3.3.4.2)$$

The heat produced is given by

$$q_j = -K\frac{\partial T}{\partial x_j} \quad (3.3.4.3)$$

K is the thermal conductivity.

The equation gives enthalpy

$$r = e + \frac{P}{\rho}\,, \quad (3.3.4.4)$$

Differentiating equation (3.3.4.4) becomes,

$$dr = de + \frac{1}{\rho}dP + Pd\left(\frac{1}{\rho}\right) \quad (3.3.4.5)$$

By the first and second laws of thermodynamics, change in specific internal energy is given by

$$de = TdS - Pd\left(\frac{1}{\rho}\right) \quad (3.3.4.6)$$

S was entropy which is a function of pressure and temperature

$$S = S(P, T). \quad (3.3.4.7)$$

Differentiating equation (3.3.4.7) gives

$$dS = \left(\frac{\partial S}{\partial P}\right)_T dP + \left(\frac{\partial S}{\partial T}\right)_P dT \quad (3.3.4.8)$$

Applying generalized thermodynamic relations $\left(\frac{\partial S}{\partial P}\right)_T = -\frac{G}{\rho}$ and $\left(\frac{\partial S}{\partial T}\right)_P = \frac{C_p}{T}$ equation (3.3.4.8) becomes

$$dS = -\frac{G}{\rho}dP + \frac{C_p}{T}dT. \quad (3.3.4.9)$$

Substituting equation (3.3.4.9) into equation (3.3.4.5)

$$dr = -\frac{G}{\rho}TdP + \frac{C_p}{T}TdT + \frac{1}{\rho}dP \quad (3.3.4.10)$$

Simplifying to

$$dr = C_p dT + \frac{1}{\rho}(1 - GT)dP \quad (3.3.4.11)$$

Substituting equation (3.3.4.11), (3.3.4.2) and (3.3.4.3) to equation (3.3.4.1)

$$\frac{\partial}{\partial t}(\rho C_p T) + \frac{\partial}{\partial x_j}(\rho C_p u_j T) = \frac{\partial}{\partial x_j}\left(K \frac{\partial T}{\partial x_j}\right) + \mu \left(\frac{\partial u}{\partial y}\right)^2 \quad (3.3.4.12)$$

In x- and z- directions, the plates have immeasurable length hence equation (3.3.4.12) becomes,

$$\rho C_p \left(\frac{\partial T}{\partial t} + v_\circ \frac{\partial T}{\partial y}\right) = K \frac{\partial^2 T}{\partial y^2} + \mu \left(\frac{\partial u}{\partial y}\right)^2 \quad (3.3.4.13)$$

Since the flow is steady, equation (3.3.4.13) results to,

$$\rho C_p v_\circ \frac{\partial T}{\partial y} = K \frac{\partial^2 T}{\partial y^2} + \mu \left(\frac{\partial u}{\partial y}\right)^2 \quad (3.3.4.14)$$

Effecting electrical resistance of the fluid due to Ohmic heating which is $\frac{J^2}{\sigma}$ equation (3.3.4.14) gives

$$\rho C_p v_\circ \frac{\partial T}{\partial y} = K \frac{\partial^2 T}{\partial y^2} + \mu \left(\frac{\partial u}{\partial y}\right)^2 + \frac{J^2}{\sigma}. \quad (3.3.4.15)$$

From equation (3.3.2.8)

$$J = \sigma U B_y.$$

So

$$\frac{J^2}{\sigma} = \frac{\sigma^2 U^2 {B_y}^2}{\sigma} = \sigma U^2 {B_y}^2. \quad (3.3.4.16)$$

But, ${B_y}^2 = {\mu_e}^2 {H_y}^2$. Therefore Ohmic heating is given by

$$\frac{J^2}{\sigma} = \sigma {\mu_e}^2 {H_y}^2 U^2 \quad (3.3.4.17)$$

Substituting equation (3.3.4.17) to equation (3.3.4.15) results to

$$\rho C_p v_\circ \frac{\partial T}{\partial y} = K \frac{\partial^2 T}{\partial y^2} + \mu \left(\frac{\partial u}{\partial y}\right)^2 + \sigma {\mu_e}^2 {H_y}^2 U^2 \qquad (3.3.4.18)$$

The initial conditions and boundary conditions used in this study were

$$\left.\begin{array}{l} \mathrm{u} = 0 \text{ when } \mathrm{t} = 0 \text{ and } -\mathrm{a} \leq \mathrm{y} \leq \text{ at } \mathrm{T} = 0 \\ \mathrm{u} = 0 \text{ when } \mathrm{t} > 0 \text{ and } \mathrm{y} = -\mathrm{a} \text{ at } \mathrm{T} = T_w \\ \mathrm{u} = \mathrm{U} \text{ when } \mathrm{t} > 0 \text{ and } \mathrm{y} = \mathrm{a} \text{ at } \mathrm{T} = T_\infty \end{array}\right\} \qquad (3.3.4.19)$$

3.4 NON-DIMENSIONALIZATION

This refers to the partial or complete elimination of units and substituting of an appropriate variable. This method communicates the nature of the model in an organized manner, consequently presenting the outcomes in the most competent, efficient, and logical way.

This study uses the following dimensionless parameters;

i. Eckert number

It refers to the relation between heat transfer and dissipation of heat. It characterizes the influence of the self-heating of a fluid as a consequence of dissipation effects. It is expressed as

$$E_C = \frac{U^2}{C_p \Delta T} \qquad (3.4.1)$$

ii. Prandtl number.

It represents the relationship between diffusion of momentum and thermal diffusivity. It calculates heat transmission involving a solid object and a flowing fluid.

$$P_r = \frac{v}{\propto} = \frac{\mu/\rho}{K/C_p\rho} = \frac{\mu}{\rho}.\frac{C_p\rho}{K} = \frac{C_p\mu}{K} \quad (3.4.2)$$

iii. Hartmann parameter

It shows the relation between viscous force and electromagnetic force. Hartmann describes the degree of significance of drag force as a result of viscous force and magnetic induction force.

$$H_a = L\mu_e H\sqrt{\frac{\sigma}{\mu}} \quad (3.4.3)$$

iv. Reynold's number

Reynold's parameter describes the relationship between viscous forces and inertial forces. It predicts turbulent and laminar fluid flow.

$$R_e = \frac{\rho uL}{\mu} \quad (3.4.4)$$

v. Suction parameter.

This is the relationship between the fluid's main velocity and the fluid's flow through the pores.

$$S_\circ = \frac{v_\circ}{u} \quad (3.4.5)$$

vi. Magnetic parameter.

This is the relationship between inertial force and electromagnetic force. It is also referred to as the Stuart number given by

$$\text{M}=\frac{\sigma\mu_e^2 H_y^2 L}{\rho U} = \frac{H_a^2}{R_e} \quad (3.4.6)$$

To non-dimensionalize the equation (3.3.3.11) and equation (3.3.4.18) and also the initial boundary conditions in equation (3.3.4.19), we use transformations below where the values with asterisks represent the dimensionless variables.

$$X^* = \frac{X}{L} \quad Y^* = \frac{Y}{L} \quad P^* = \frac{P}{\rho u^2} \quad u^* = \frac{u}{U} \quad T^* = \frac{T-T_\infty}{T_{W-T_\infty}} \quad t^* = \frac{tU}{L} \tag{3.4.7}$$

The following analysis was carried out using the above transformations in the equation.

$$\frac{\partial u}{\partial y} = \frac{\partial y^*}{\partial y}\frac{\partial u^*}{\partial y^*}\frac{\partial u}{\partial u^*} = \frac{\partial u^*}{\partial y^*}\frac{U}{L} \tag{3.4.8}$$

$$\frac{\partial^2 u}{\partial y^2} = \frac{\partial}{\partial y^*}\left(\frac{\partial u}{\partial y}\right)\frac{\partial y^*}{\partial y} = \frac{\partial}{\partial y^*}\left(\frac{U}{L}\frac{\partial u^*}{\partial y^*}\right)\frac{1}{L} = \frac{U}{L^2}\frac{\partial^2 u^*}{\partial y^{*2}} \tag{3.4.9}$$

$$\frac{\partial P}{\partial X} = \frac{\partial X^*}{\partial X}\frac{\partial P^*}{\partial X^*}\frac{\partial P}{\partial P^*} = \frac{\rho U^2}{L}\frac{\partial P^*}{\partial X^*} \tag{3.4.10}$$

$$\frac{\partial T}{\partial y} = \frac{\partial y^*}{\partial y}\frac{\partial T^*}{\partial y^*}\frac{\partial T}{\partial T^*} = \frac{(T_W-T_\infty)}{L}\frac{\partial T^*}{\partial y^*} \tag{3.4.11}$$

$$\frac{\partial^2 T}{\partial y^2} = \frac{\partial}{\partial y^*}\left(\frac{\partial T}{\partial y}\right)\frac{\partial y^*}{\partial y} = \frac{\partial}{\partial y^*}\left(\frac{(T_W-T_\infty)}{L}\frac{\partial T^*}{\partial y^*}\right)\frac{1}{L} = \frac{(T_W-T_\infty)}{L^2}\frac{\partial^2 T^*}{\partial y^{*2}} \tag{3.4.12}$$

Substituting these equations (3.4.8) - (3.4.12) to equation (3.3.3.11)

$$v_\circ \frac{\partial u}{\partial y} = -\frac{1}{\rho}\frac{\partial P}{\partial x} + \frac{\mu}{\rho}\frac{\partial^2 u}{\partial y^2} - \frac{U\sigma\mu_e^2 H_y^2}{\rho}$$

It becomes

$$v_\circ \frac{U}{L}\frac{\partial u^*}{\partial y^*} = -\frac{1}{\rho}\frac{\rho U^2}{L}\frac{\partial P^*}{\partial X^*} + \frac{\mu}{\rho}\frac{U}{L^2}\frac{\partial^2 u^*}{\partial y^{*2}} - \frac{\sigma U U^* \mu_e^2 H_y^2}{\rho} \tag{3.4.13}$$

Multiplying both sides of the equation (3.4.13) by $\frac{L}{U^2}$ we get

$$v_\circ \frac{U}{L}\frac{L}{U^2}\frac{\partial u^*}{\partial y^*} = -\frac{1}{\rho}\frac{\rho U^2}{L}\frac{L}{U^2}\frac{\partial P^*}{\partial X^*} + \frac{\mu}{\rho}\frac{U}{L^2}\frac{L}{U^2}\frac{\partial^2 u^*}{\partial y^{*2}} - \frac{\sigma U U^* \mu_e^2 H_y^2}{\rho}\frac{L}{U^2} \quad (3.4.14)$$

Simplifying to

$$\frac{v_\circ}{U}\frac{\partial u^*}{\partial y^*} = -\frac{\partial P^*}{\partial X^*} + \frac{\mu}{\rho L U}\frac{\partial^2 u^*}{\partial y^{*2}} - \frac{\sigma \mu_e^2 H_y^2 L}{\rho U} U^* \quad (3.4.15)$$

Substituting the dimensionless numbers to equation (3.4.15) results to

$$S_\circ \frac{\partial u^*}{\partial y^*} = -\frac{\partial P^*}{\partial X^*} + \frac{1}{R_e}\frac{\partial^2 u^*}{\partial y^{*2}} - \frac{H_a^2}{R_e} U^* \quad (3.4.16)$$

Simplifying to

$$S_\circ \frac{\partial u^*}{\partial y^*} = -\frac{\partial P^*}{\partial X^*} + \frac{1}{R_e}\frac{\partial^2 u^*}{\partial y^{*2}} - M U^* \quad (3.4.17)$$

Similarly, substituting the equations (3.4.8) - (3.4.12) to equation (3.3.4.18)

$$\rho C_p v_\circ \frac{\partial T}{\partial y} = K\frac{\partial^2 T}{\partial y^2} + \mu\left(\frac{\partial u}{\partial y}\right)^2 + \sigma {\mu_e}^2 {H_y}^2 U^2$$

We got

$$\rho C_p v_\circ \frac{(T_W - T_\infty)}{L}\frac{\partial T^*}{\partial y^*} = K\frac{(T_W - T_\infty)}{L^2}\frac{\partial^2 T^*}{\partial y^{*2}} + \mu\left(\frac{U}{L}\frac{\partial u^*}{\partial y^*}\right)^2 + \sigma {\mu_e}^2 {H_y}^2 U^2 U^{*2} \quad (3.4.18)$$

Multiplying both sides of the equation (3.4.16) by $\frac{L}{U\Delta T}$ becomes

$$\rho C_p v_\circ \frac{L}{U\Delta T}\frac{(T_W - T_\infty)}{L}\frac{\partial T^*}{\partial y^*} =$$

$$K\frac{L}{U\Delta T}\frac{(T_W - T_\infty)}{L^2}\frac{\partial^2 T^*}{\partial y^{*2}} + \mu\frac{L}{U\Delta T}\left(\frac{U}{L}\frac{\partial u^*}{\partial y^*}\right)^2 + \sigma {\mu_e}^2 {H_y}^2 U^2 U^{*2}\frac{L}{U\Delta T} \quad (3.4.19)$$

This simplifies to

$$\frac{\rho C_p v_\circ}{U\Delta T}(T_W - T_\infty)\frac{\partial T^*}{\partial y^*} = K\frac{(T_W - T_\infty)}{LU\Delta T}\frac{\partial^2 T^*}{\partial y^{*2}} + \frac{\mu U}{L\Delta T}\left(\frac{\partial u^*}{\partial y^*}\right)^2 + \frac{\sigma {\mu_e}^2 {H_y}^2 U U^{*2} L}{\Delta T} \quad (3.4.20)$$

We multiply equation (3.4.20) by $\frac{1}{\rho C_p}$ and consider $\Delta T = T_W - T_\infty$ obtaining

$$\frac{v_\circ}{U}\frac{\partial T^*}{\partial y^*} = \frac{K}{\rho L U C_p}\frac{\partial^2 T^*}{\partial y^{*2}} + \frac{\mu U}{L\Delta T\rho C_p}\left(\frac{\partial u^*}{\partial y^*}\right)^2 + \frac{L\sigma U {\mu_e}^2 {H_y}^2}{\Delta T\rho C_p}U^{*2} \quad (3.4.21)$$

Substituting the dimensionless numbers equation (3.4.21) results to

$$S_\circ\frac{\partial T^*}{\partial y^*} = \frac{1}{R_e P_r}\frac{\partial^2 T^*}{\partial y^{*2}} + \frac{E_C}{R_e}\left(\frac{\partial u^*}{\partial y^*}\right)^2 + \frac{E_C {H_a}^2}{R_e}U^{*2} \quad (3.4.22)$$

Non- dimensionalizing the initial boundary conditions in equation (3.3.4.19)

At t$\leq$ 0, $t^* = \frac{t}{T} = 0$ and $t > 0$, $t^* > 0$

At $T = T_W$, $\frac{T - T_\infty}{T_W - T_\infty} = T^* = 1$ and $T = T_W$, $\frac{T_\infty - T_\infty}{T_W - T_\infty} = T^* = 0$

At $u = 0$, $u^* = \frac{u}{U} = 0$ and $u > U$, $\frac{U}{U} = u^* = 1$

At $y = -a$, $y^* = \frac{y}{L} = -\frac{L}{L} = -1$ and $y = a$, $y^* = \frac{L}{L} = 1$

Non- dimensionalized initial conditions and boundary conditions become

$$t^* = 0, u^* = 0,\ T^* = 0\ , at - 1 \leq y^*\ \leq 1 \quad (3.4.23)$$

$$t^* > 0, u^* = 0, T^* = 1\ at\ y^* = -1$$

$$t^* > 0, u^* = 1, T^* = 0\ at y^* = 1$$

CHAPTER FOUR

METHODOLOGY

Finite Difference Method (FDM)

FDM reduces PDE$_S$ into algebraic matrix equations, which can be solved using computer software. The governing PDE$_s$ were presented in their finite difference approximations and then used FDM. For simplicity, we consider a 1D domain (space). Derivative of u with respect to t was given by,

$$\frac{\partial u}{\partial t} = u_t = \lim_{\Delta t \to 0} \frac{-u(t,y)+u(t+\Delta t),u(y)}{\Delta t}. \quad (4.1.1)$$

From the Taylors series,

$$u(y+\Delta y) = u(y) + \Delta y u_y(y) + \frac{\Delta y^2}{2!}u_{yy} + \cdots + \frac{\Delta y^{n-1}}{(n-1)!}u_{n-1} + 0(\Delta y^n). \quad (4.1.2)$$

Truncating equation (4.1.2) to $0(\Delta y^2)$ gives

$$u(y+\Delta y) = u(y) + \Delta y u_y(y) + 0(\Delta y^2). \quad (4.1.3)$$

Rearranging equation (4.1.3), we got finite difference approximation to partial derivatives

$$u_y(y) = -\frac{0(\Delta y^2)}{\Delta y} + \frac{-u(y)+u(y+\Delta y)}{\Delta y} \quad (4.1.4)$$

Obtaining

$$u_y(y) = -0(\Delta y) + \frac{-u(y)+u(y+\Delta y)}{\Delta y} \quad (4.1.5)$$

Equation (4.1.5) holds at any point y.

Figure 4.1 mesh grid

We consider a rectangular mesh grid with space variable (y) on the horizontal axis and time variable (t) on the vertical axis. The approximations of solutions were computed at mesh points (j, k) which gave the space-time references. Figure 4.1 gives approximations of mesh points of space and time variables. We write partial derivatives of the mesh points using the forward-time backward space finite difference method. For instance, u_t On average, for times k, k+1 is given by

$$\frac{\partial u}{\partial t} = \frac{u_j^{k+1} - u_j^k}{\Delta t} + 0(\Delta t). \qquad (4.1.6)$$

The finite difference expressions for U and T in equations were

$$\frac{\partial u^*}{\partial y^*} = \frac{U_j^{k+1} - U_{j-1}^{k+1} + U_j^k - U_{j-1}^k}{2\Delta y} \tag{4.1.7}$$

$$\frac{\partial^2 u^*}{\partial y^{*2}} = \frac{U_{j+1}^{k+1} + U_{j+1}^k - 2U_j^{k+1} - 2U_j^k + U_{j-1}^k + U_{j-1}^{k+1}}{2(\Delta y)^2} \tag{4.1.8}$$

$$\frac{\partial T^*}{\partial y^*} = \frac{T_j^{k+1} - T_{j-1}^{k+1} + T_j^k - T_{j-1}^k}{2\Delta y} \tag{4.1.8}$$

$$\frac{\partial^2 T^*}{\partial y^{*2}} = \frac{T_{j+1}^{k+1} + T_{j+1}^k - 2T_j^{k+1} - 2T_j^k + T_{j-1}^k + T_{j-1}^{k+1}}{2(\Delta y)^2} \tag{4.1.9}$$

Equations (4.1.7) and (4.1.8) were substituted to equation (3.4.17)

$$S_\circ \left(\frac{U_j^{k+1} - U_{j-1}^{k+1} + U_j^k - U_{j-1}^k}{2\Delta y} \right) =$$

$$-\frac{\partial P^*}{\partial X^*} + \frac{1}{R_e}\left(\frac{U_{j+1}^{k+1} - 2U_j^{k+1} + U_{j-1}^{k+1} + U_{j+1}^k - 2U_j^k + U_{j-1}^k}{2(\Delta y)^2} \right) - MU_j^k \tag{4.1.10}$$

Rearranging to get

$$0 = -\frac{\partial P^*}{\partial X^*} - S_\circ \left(\frac{U_j^{k+1} - U_{j-1}^{k+1} + U_j^k - U_{j-1}^k}{2\Delta y} \right)$$

$$+ \frac{1}{R_e}\left(\frac{U_{j+1}^{k+1} - 2U_j^{k+1} + U_{j-1}^{k+1} + U_{j+1}^k - 2U_j^k + U_{j-1}^k}{2(\Delta y)^2} \right) - MU_j^k \tag{4.1.11}$$

Making U_j^{k+1} the subject of the formula

$$\left[\frac{S_\circ}{2\Delta y} + \frac{1}{R_e(\Delta y)^2} \right] U_j^{k+1} = -\frac{\partial P^*}{\partial X^*} - S_\circ \left(\frac{U_j^k - U_{j-1}^{k+1} - U_{j-1}^k}{2\Delta y} \right) + \frac{1}{R_e}\left(\frac{U_{j+1}^{k+1} + U_{j-1}^{k+1} + U_{j+1}^k - 2U_j^k + U_{j-1}^k}{2(\Delta y)^2} \right) -$$

$$MU_j^k \tag{4.1.12}$$

$$U_j^{k+1} = \left\{ -\frac{\partial P^*}{\partial X^*} - S_\circ \left(\frac{U_j^k - U_{j-1}^{k+1} - U_{j-1}^k}{2\Delta y} \right) + \frac{1}{R_e} \left(\frac{U_{j+1}^{k+1} + U_{j-1}^{k+1} + U_{j+1}^k - 2U_j^k + U_{j-1}^k}{2(\Delta y)^2} \right) - MU_j^k \right\} \div$$

$$\left(\frac{S_\circ}{2\Delta y} + \frac{1}{R_e(\Delta y)^2} \right) \quad (4.1.13$$

Equation (4.1.9) and equation (4.1.8) are substituted to equation (3.4.22)

$$S_\circ \left(\frac{T_j^{k+1} - T_{j-1}^{k+1} + T_j^k - T_{j-1}^k}{2\Delta y} \right) = \frac{1}{R_e P_r} \left(\frac{T_{j+1}^{k+1} - 2T_j^{k+1} + T_{j-1}^{k+1} + T_{j+1}^k - 2T_j^k + T_{j-1}^k}{2(\Delta y)^2} \right) +$$

$$\frac{E_C}{R_e} \left(\frac{U_{j+1}^{k+1} - 2U_j^{k+1} + U_{j-1}^{k+1} + U_{j+1}^k - 2U_j^k + U_{j-1}^k}{2(\Delta y)^2} \right) + \frac{E_C {H_a}^2}{R_e} \left(U_j^k \right)^2$$

(4.1.14)

Making T_j^{k+1} the formula of subject

$$\left(\frac{S_\circ}{2\Delta y} + \frac{1}{R_e P_r (\Delta y)^2} \right) T_j^{k+1} = -S_\circ \left(\frac{T_j^k - T_{j-1}^{k+1} - T_{j-1}^k}{2\Delta y} \right) + \frac{1}{R_e P_r} \left(\frac{T_{j-1}^{k+1} + T_{j+1}^{k+1} + T_{j-1}^k - 2T_j^k + T_{j+1}^k}{2(\Delta y)^2} \right) +$$

$$\frac{E_C}{R_e} \left(\frac{U_{j+1}^{k+1} + U_{j-1}^{k+1} + U_{j+1}^k - 2U_j^k + U_{j-1}^k}{2(\Delta y)^2} \right) + \frac{E_C {H_a}^2}{R_e} \left(U_j^k \right)^2 \quad (4.1.15)$$

$$T_j^{k+1} = \left\{ -S_\circ \left(\frac{T_j^k - T_{j-1}^{k+1} - T_{j-1}^k}{2\Delta y} \right) + \frac{1}{R_e P_r} \left(\frac{T_{j-1}^{k+1} + T_{j+1}^{k+1} + T_{j-1}^k - 2T_j^k + T_{j+1}^k}{2(\Delta y)^2} \right) + \right.$$

$$\left. \frac{E_C}{R_e} \left(\frac{U_{j+1}^{k+1} - 2U_j^{k+1} + U_{j-1}^{k+1} + U_{j+1}^k - 2U_j^k + U_{j-1}^k}{2(\Delta y)^2} \right) + \frac{E_C {H_a}^2}{R_e} \left(U_j^k \right)^2 \right\} \div \left(\frac{S_\circ}{2\Delta y} + \frac{1}{R_e P_r (\Delta y)^2} \right) \quad (4.1.16)$$

Simultaneously, we solve equation (4.1.13) and equation (4.1.16) using matrix laboratory (R2018b) computer software.

CHAPTER FIVE

RESULTS AND DISCUSSION

Introduction

Effects of variable pressure gradient on Magnetohydrodynamic flow between parallel plates considering variable transverse magnetic fields were investigated. The results were presented graphically using MATLAB (R2018b) computer software and discussed different parameters. Default values were chosen to observe the effect on varying parameter values. In this study, the default parameter values considered were:

$$p_g = -200, S_\circ = 450, R_e = 1.25, P_r = 0.06, E_C = 0.03, H_a = 1.1, M = 9.5$$

5.1 Outcome of Reynold's number on temperature and velocity profiles

We varied Reynold's number (R_e) as $R_e = 1.25,2.25,3.25,4.25$. The obtained results were presented graphically. All other variables were held constant.

Figure 5.1a shows that the velocity of the flow decreased as Reynold's number increased. Since Reynold's number is the ratio of inertial forces to viscous forces, an increase in Reynold's number implies that viscous forces decrease as inertial forces increase hence reducing velocity. Viscous force is inversely proportional to inertia force, implying that an increase in Reynold's parameter causes a reduction of the velocity of the fluid.

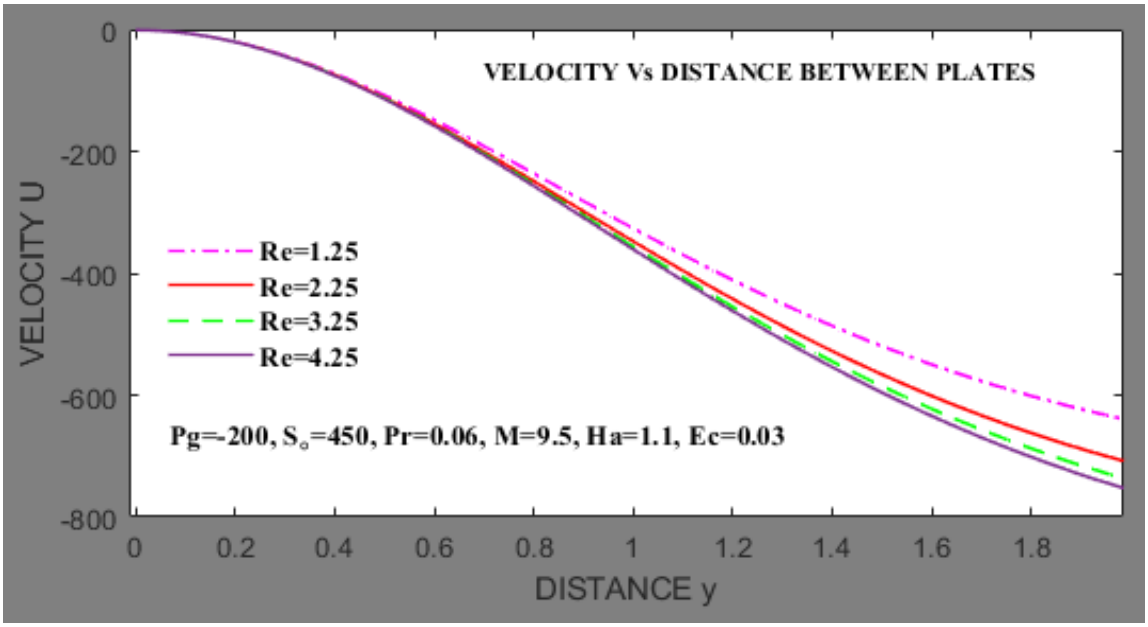

Figure 5.1a: Outcome of Reynold's number on the velocity of the fluid

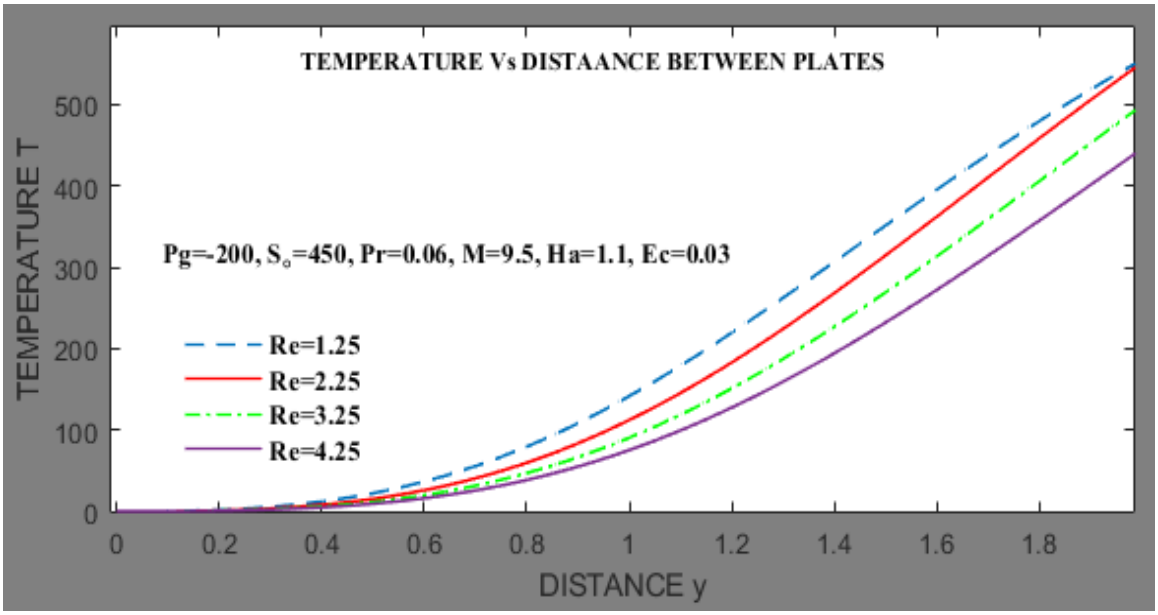

Figure 5.1b: Outcome of Reynold's number on the temperature of the fluid

From figure 5.1b, temperature decreases as the Reynolds number rises. Decreased viscous forces imply that friction force lessens, so the fluid temperature goes down, Bafakeeh *et al*. (2022).

5.2 Outcome of Prandtl parameter on temperature and velocity profiles

Prandtl number (P_r) was varied as $P_r = 0.06,0.07,0.08,0.09$. The obtained results were presented graphically. All other variables were held constant.

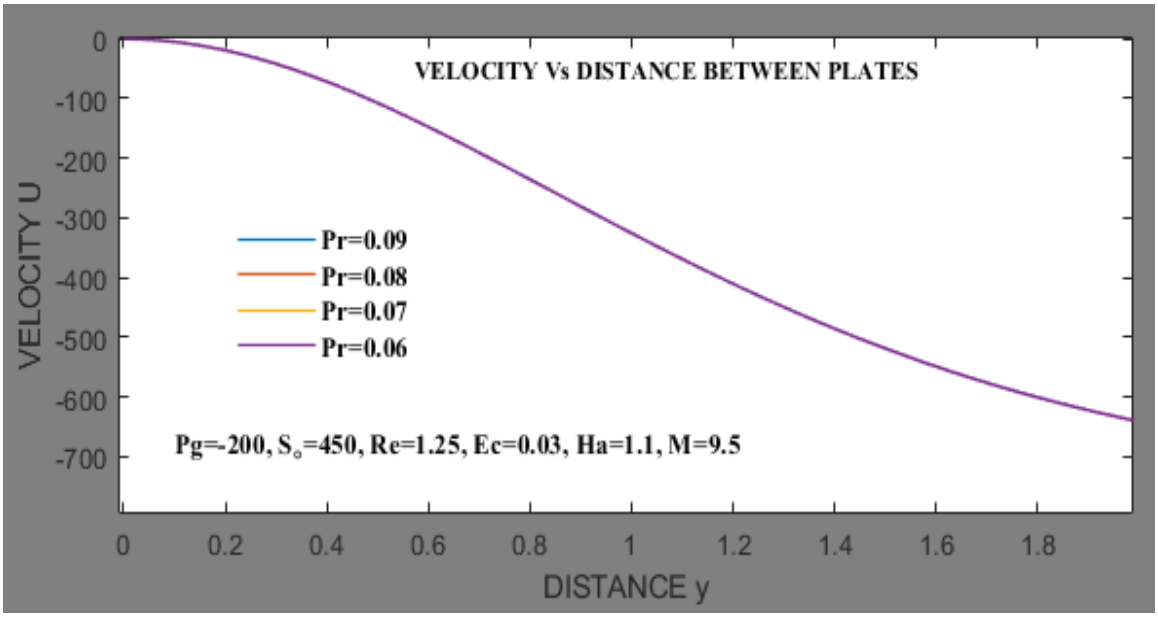

Figure 5.2a: Outcome of Prandtl parameter on the velocity of the fluid

From figure 5.2a above, an increase in the Prandtl number did not affect velocity profiles. Prandtl number focuses on momentum diffusivity and thermal diffusivity Animasaun *et al*. (2022). Thermal exchanges affect the fluid's temperature; hence no effect on velocity.

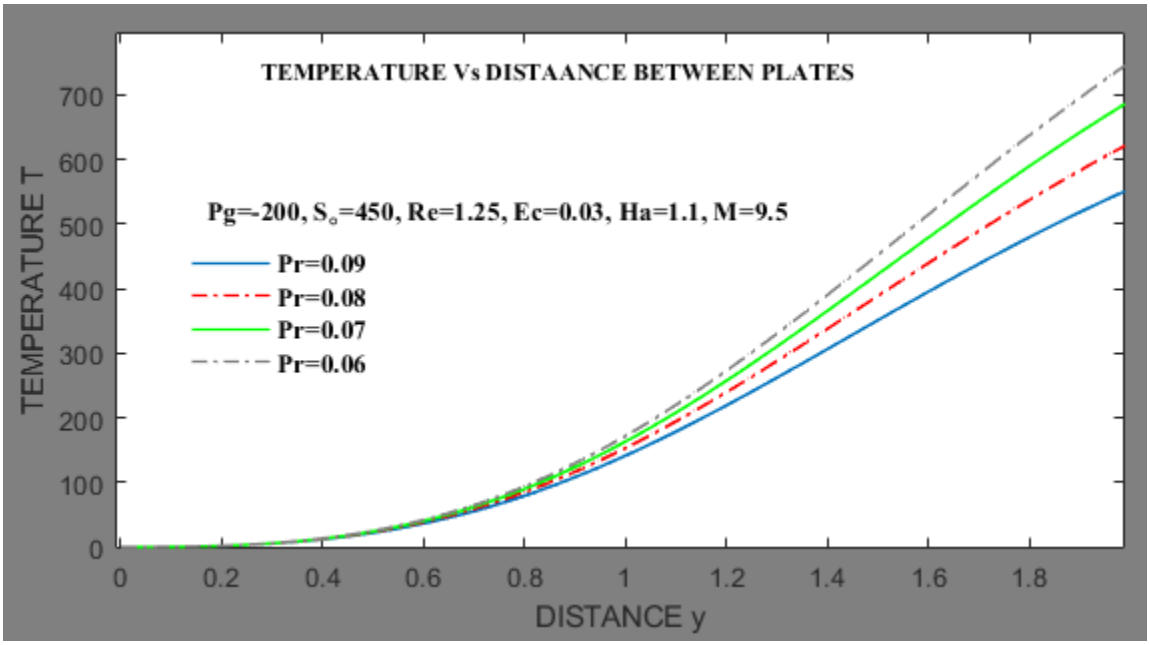

Figure 5.2b: Outcome of Prandtl parameter on the temperature of the fluid

In figure 5.2b, increased Prandtl parameter led to reduced temperature. Prandtl describes the relationship between thermal diffusion and momentum diffusivity. Momentum diffusivity dominates when the Prandtl number is higher hence reduced thermal conductivity resulting in decreased thermal boundary thickness consequently decrease in temperature.

5.3 Outcome of Pressure gradient on temperature and velocity profiles

Pressure gradient (p_g) was varied as $p_g = -180, -185, -190, -200$ .The obtained results are presented graphically. The negative sign on the pressure gradient indicates that pressure acts in the same direction as fluid flow. All other variables were held constant.

Figure 5.3a below implied that the velocity of the fluid reduced as the pressure gradient increased. It was observed that at the stationary bottom plate, the flow assumed the velocity of the plate Turkyilmazoglu (2021). The velocity rises gradually to the

maximum as it reaches the center of the two plates, then decreases as it approaches the top plate.

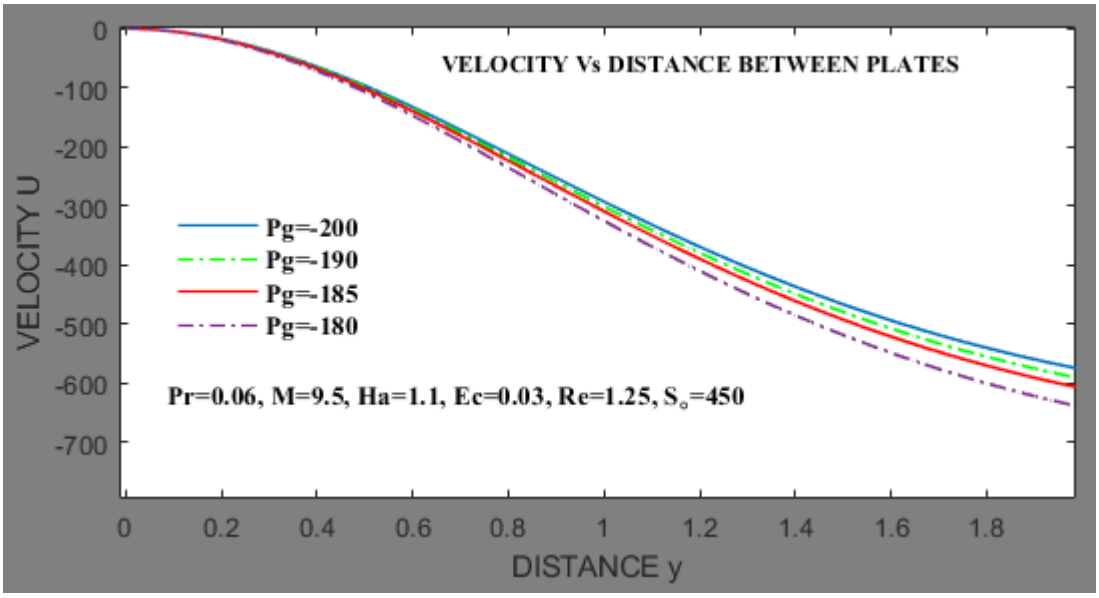

Figure 5.3a: Outcome of pressure gradient on the velocity of the fluid

Figure 5.3b shows that as the pressure gradient increases, the temperature of the fluid rises.

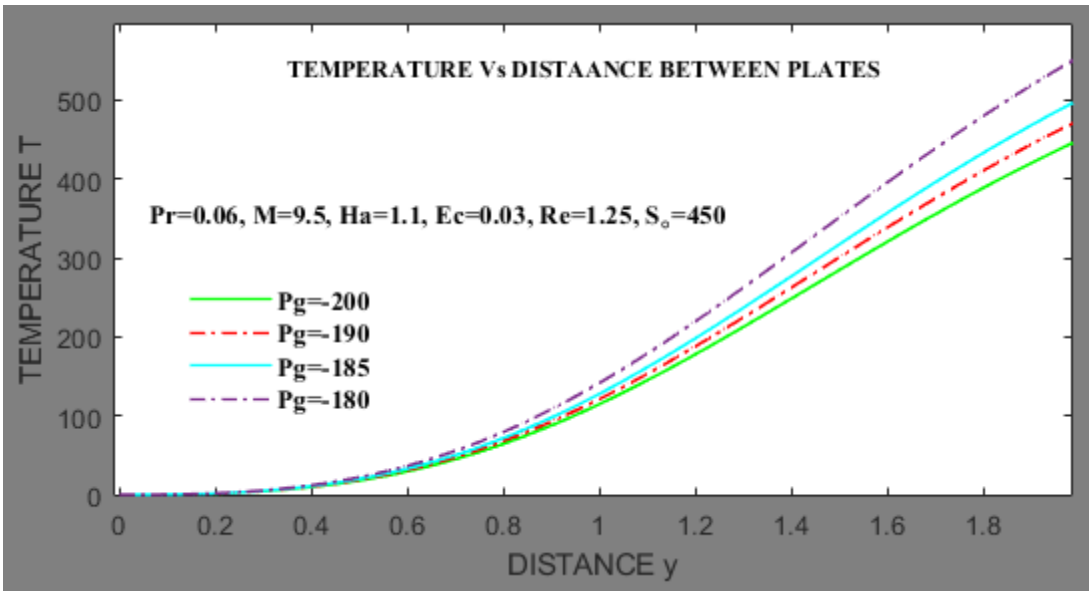

Figure 5.3b outcomes of pressure gradient on the temperature of the fluid

5.4 Outcome of the magnetic number on temperature and velocity profiles

Magnetic number (M) was varied as $M = 9.5,9.6,9.7,9.8$. The obtained results are presented graphically. All other variables were held constant.

From figure 5.4a below, a rising magnetic number lowers the velocity of the fluid. Lorentz's force, generally acting on the fluid due to the influence of magnetic fields, causes resistance to the fluid flow, slowing the fluid motion and reducing the flow's velocity.

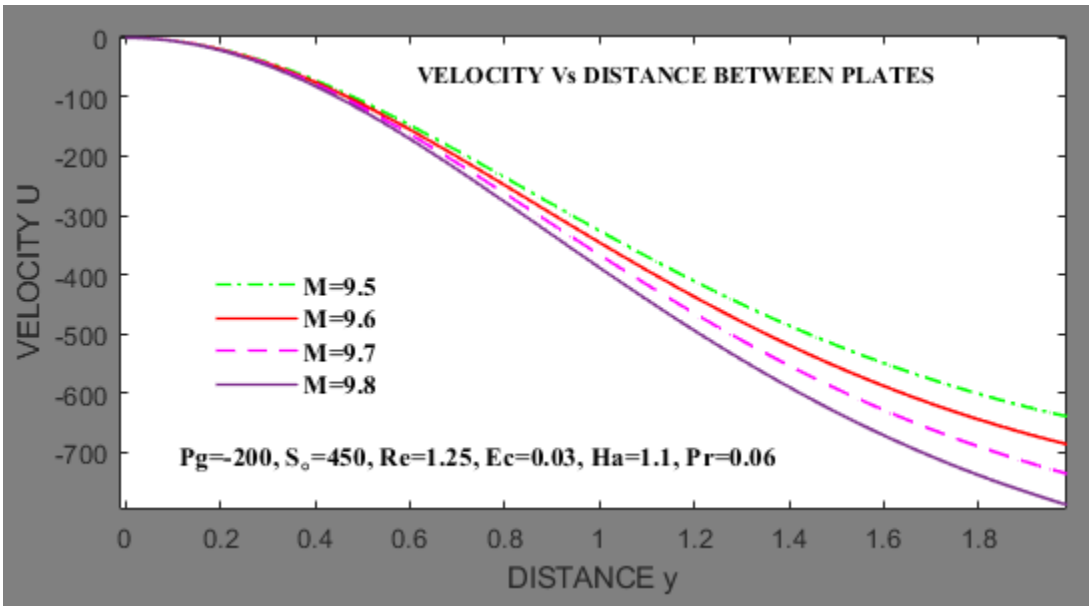

Figure 5.4a: Outcome of the magnetic number on the velocity of the fluid

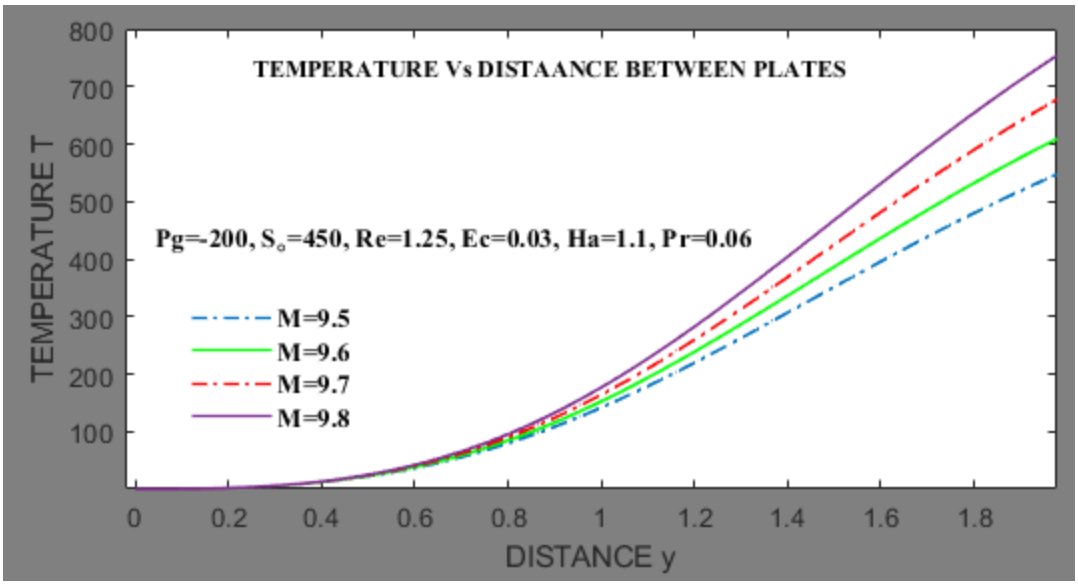

Figure 5.4b: Outcome of the magnetic number on the temperature of the fluid

From figure 5.4b, the temperature of the fluid increases when the magnetic number is raised. An increase in electromagnetic forces results in increased joule dissipation, increasing the fluid temperature Khan *et al.* (2022).

5.5 Outcome of Hartmann number on temperature and velocity profiles

Hartmann number (H_a) was varied as $H_a = 1.1,1.2,1.3,1.4$. The obtained results are presented graphically. All other variables were held constant.

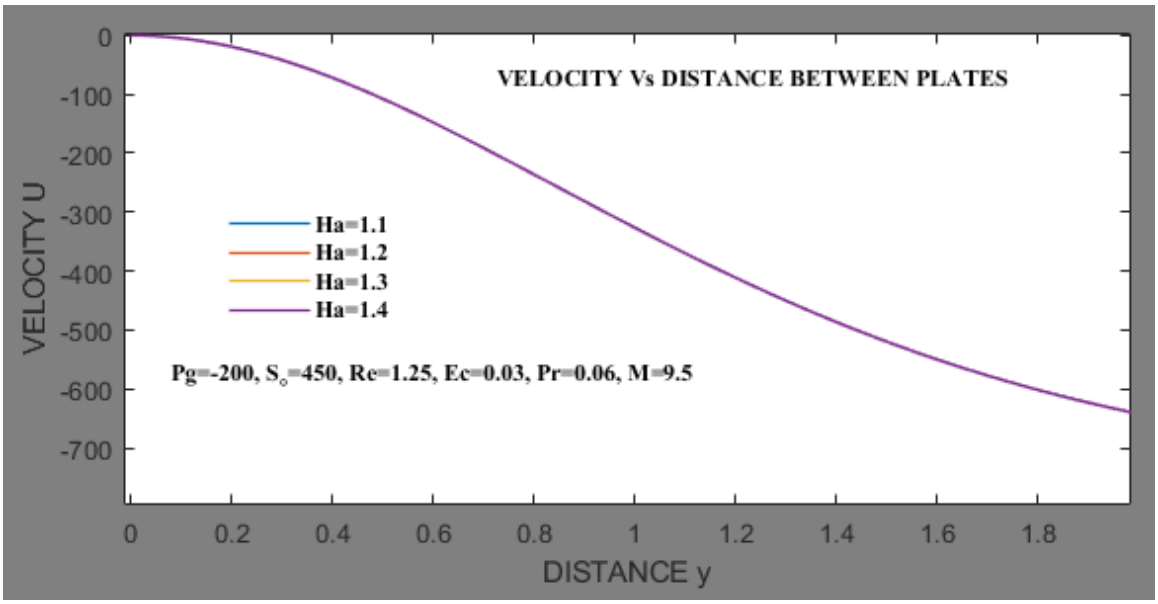

Figure 5.5a: Outcome of Hartmann number on the velocity of the fluid

From figure 5.5a above, the increase in Hartmann number did not affect the velocity profiles, Yasmeen *et al.* (2019). This is due to the presence of magnetic parameters.

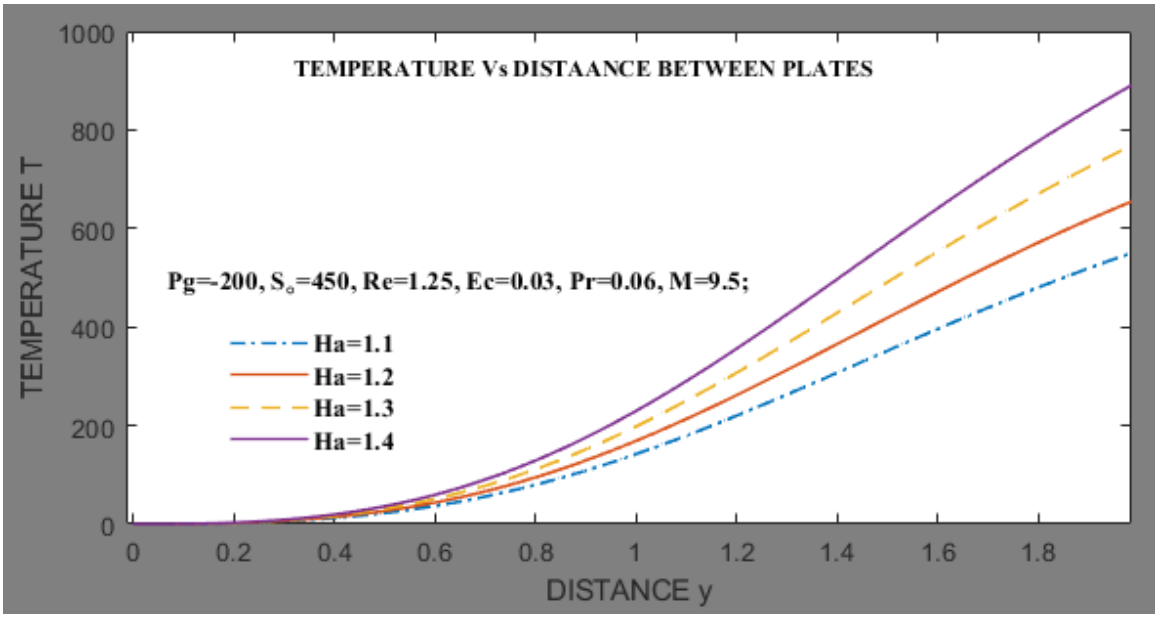

Figure5.5b: Outcome of Hartmann number on the temperature of the fluid

Figure 5.5b above describes how the temperature of the fluid increased when the Hartmann number was stepped up. An increase in Hartmann number increases joule dissipation hence higher temperatures.

5.6 Outcome of Eckert number on temperature and velocity profiles

Eckert number (E_C) was varied as $E_C = 0.03,0.04,0.05,0.06$. The obtained results are presented graphically. All other variables were held constant.

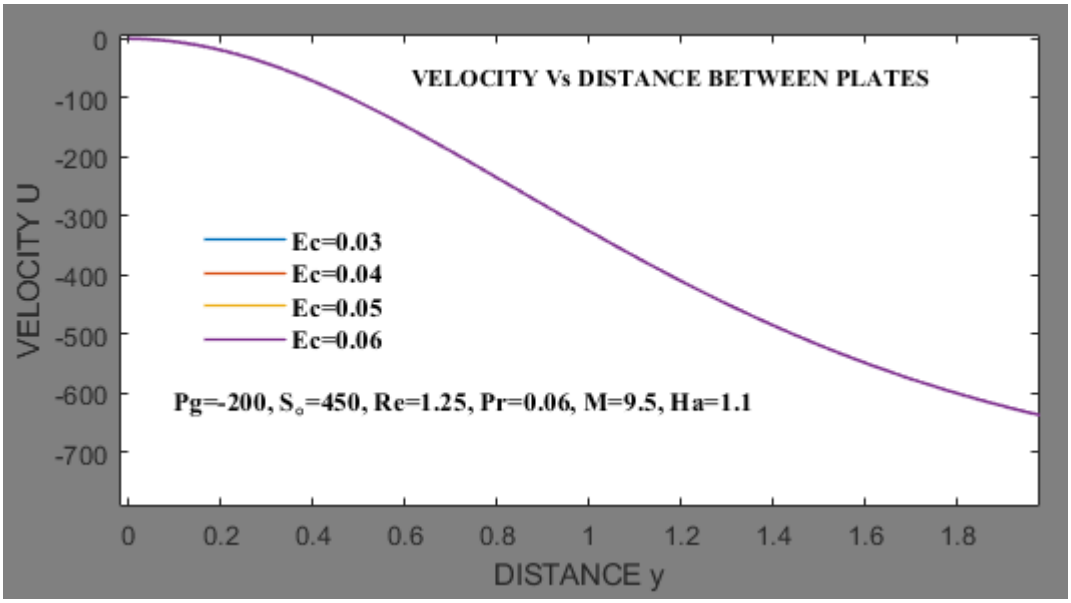

Figure 5.6a: Outcome of Eckert number on the velocity of the fluid

Figure 5.6a above implied that the increase in Eckert number did not affect velocity profiles. Eckert number affects thermal variations between the fluid boundary layer and does not affect the fluid's velocity.

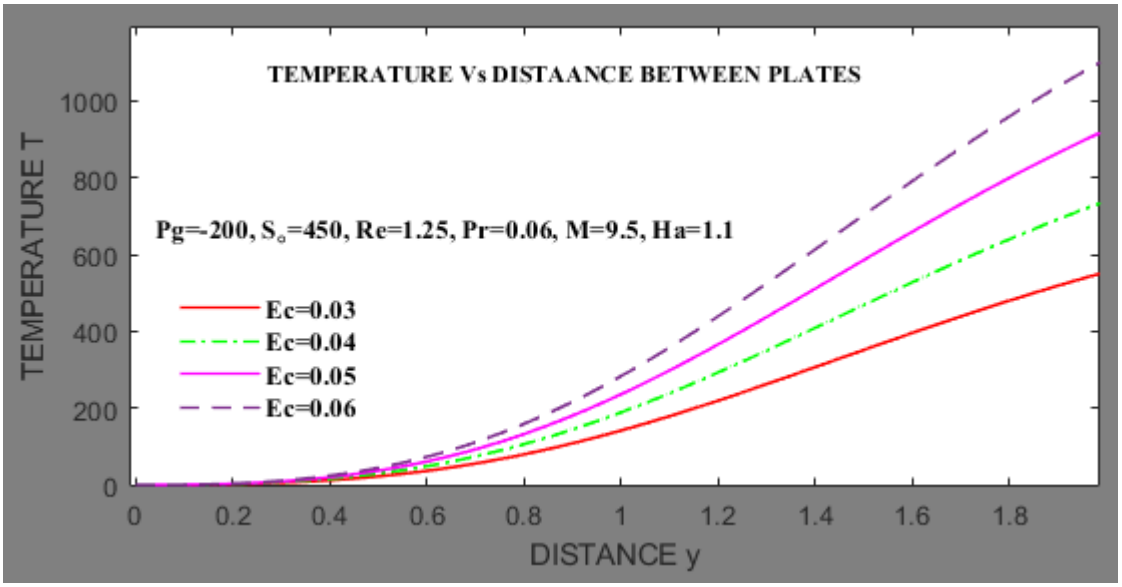

Figure 5.6b: Outcome of Eckert number on the temperature of the fluid

From figure 5.6b, as the Eckert number increased, the temperature profiles of the fluid increased. Rising Eckert number values increase the kinetic energy of the molecules; hence molecule collisions are more vigorous Zhang *et al.* (2022). An increase in collisions leads to heat disintegration in the bounded layer, consequently increasing the fluid temperature.

5.7 Outcome of suction parameter on temperature and velocity profiles

Suction number ($S_\circ$) was varied as $S_\circ = 450,452,454,456$. The obtained results are presented graphically. All other variables were held constant.

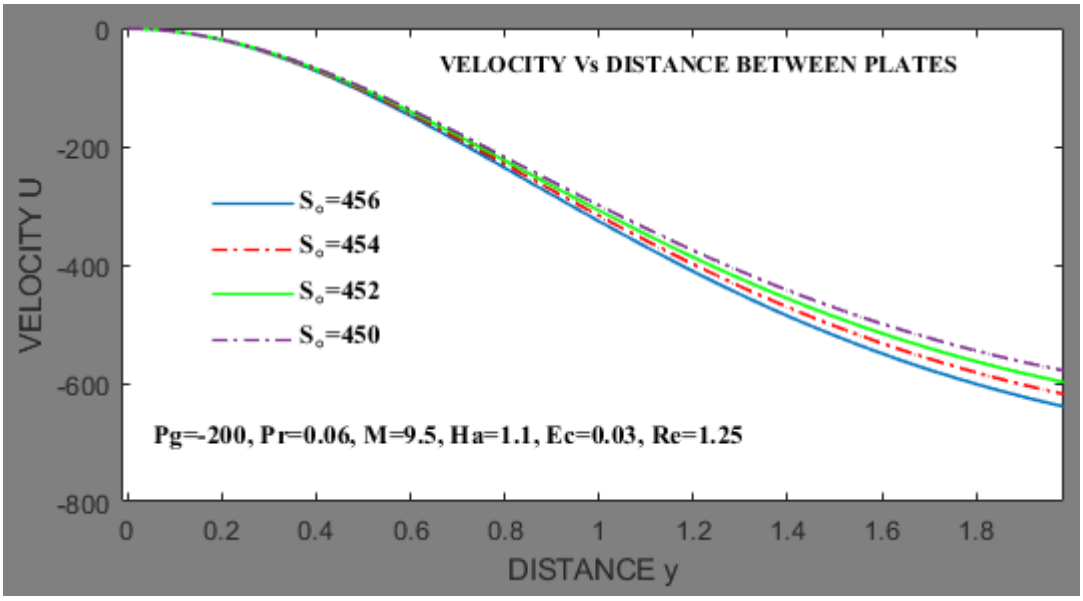

Figure 5.7a: Outcome of suction parameter on the velocity of the fluid

Figure 5.7a showed the velocity distribution of the fluid is increased by rising suction parameter values. The pressure of the fluid reduces due to the convection of the fluid particles on the surface of the plates Firdous *et al.* (2020). Reduced pressure results in decreased velocity.

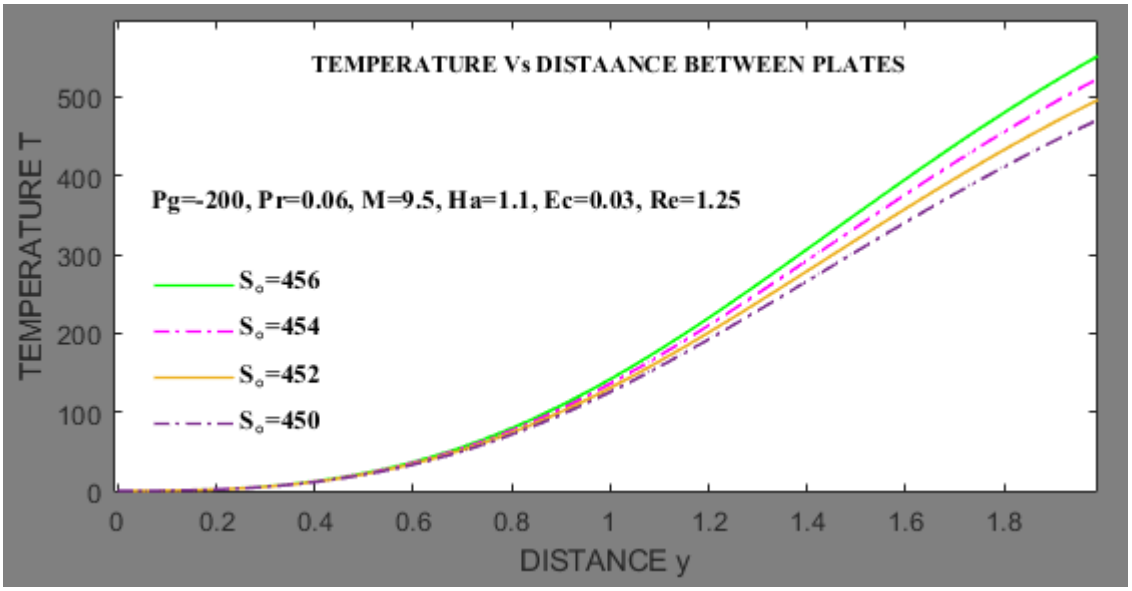

Figure 5.7b: Outcome of suction parameter on the temperature of the fluid

Figure 5.7b shows that the rising suction parameter increases the temperature profile. An increase in suction number decreases the boundary layer region, increasing the fluid's temperature gradient at the surface.

CHAPTER SIX

RECOMMENDATION AND CONCLUSION

a. CONCLUSION

The effect of variable pressure gradient on the magnetohydrodynamic flow between two parallel plates considering variable transverse magnetic fields was studied. This work has tried to determine the outcome of varying suction parameters, Eckert number, pressure gradient, magnetic parameter, Prandtl parameter, Hartmann number, and Reynalds number on temperature profile and velocity distribution. Conclusions deduced from the results of this study are;

a) Prandtl number affects the temperature of the fluid. Increasing the Prandtl number led to a decreased temperature profile.
b) An increase in magnetic parameters reduces the velocity of the fluid and raises the fluid's temperature.
c) A Higher Eckert number can lead to a more significant temperature profile. Varying Eckert's number does not affect the velocity of the fluid.
d) The suction number has to be increased for the velocity profile to decrease. However, a higher suction number results in higher temperatures.
e) Also, a rising Reynold's parameter decreases the velocity of the fluid, while a greater Reynold's parameter can lead to reduced temperatures.
f) The velocity of the flow can be decreased whenever the pressure gradient is increased. An increase in pressure gradient can result in to rise in fluid's temperature.
g) Increased Hartmann number results in a higher temperature profile.

The results obtained in this research provide valuable information to different fields, especially in designing and modeling systems in dyeing industries, cooling of automobile moving parts, and extraction of metal industries. Moreover, the findings apply to Magnetodydrodynamic flow through a porous medium, widely used in magnetohydrodynamic power generators, aerodynamic heating, and separation of matter from liquids mixed using a centrifugal separator.

b. RECOMMENDATIONS

All the areas of magnetohydrodynamic fluid flow through parallel plates were not studied exhaustively. Other areas that can be considered for further research include;

a) Variable suction.

b) Compressible and unsteady flow.

c) A compressible and steady flow

d) MHD flow between two porous plates under the influence transverse magnetic field in three dimensions.

e) Variable inclined magnetic fields.

REFERENCES

Animasaun, I. L., Shah, N. A., Wakif, A., Mahanthesh, B., Sivaraj, R., & Koriko, O. K. (2022). *Ratio of momentum diffusivity to thermal diffusivity: introduction, meta-analysis, and scrutinization*. CRC Press.

Aruna, S., and Dubewar, A. V. (2019). MHD flow between two parallel plates under the influence of an inclined magnetic field by finite difference method. *International Journal of Innovative Technology and Exploring Engineering*, 8(12), October 2019.

Bafakeeh, O. T., Raghunath, K., Ali, F., Khalid, M., Tag-ElDin, E. S. M., Oreijah, M., ... & Khan, M. I. (2022). Hall Current and Soret Effects on Unsteady MHD Rotating Flow of Second-Grade Fluid through Porous Media under the Influences of Thermal Radiation and Chemical Reactions. *Catalysts*, *12*(10), 1233.

Dash, G. C., & Ojha, K. L. (2018). Viscoelastic hydromagnetic flow between two porous parallel plates in the presence of sinusoidal pressure gradient. *Alexandria Engineering Journal*, 57(4), 3463-3471.

Firdous, H., Husnine, S. M., Hussain, F., & Nazeer, M. (2020). Velocity and thermal slip effects on two-phase flow of MHD Jeffrey fluid with the suspension of tiny metallic particles. *Physica Scripta*, *96*(2), 025803.

Ganesh, S., & Krishnambal, S. (2007). Unsteady magnetohydrodynamic stoke flow of viscous fluid between two parallel porous plates. *Journal of Applied Sciences*, 7, 374-379.

Gupta, A. S. (1975). Hydromagnetic flow past a porous flat plate with Hall Effects. *Acta Mechanica*, 22 (3-4), 281-287.

Hassanien, I. A. (1991). Unsteady hydromagnetic flow through a porous medium between two infinite parallel porous plates with time-varying suction. *Astrophysics and Space Science*, 175(1), 135-147.

Jat, R. N., & Jhankal, A. K. (2003). Three-dimensional free convective MHD flow and heat transfer through a porous medium. *Indian.Engg.Mat.SC.*, 10, 138-142.

Jones, J. R., & Walters, T. S. (1967). Flow of elastico-viscous liquids in channels under the influence of a periodic pressure gradient, part 1. *Rheologica Acta*, *6*(3), 240-245.

Joseph, K. M., Daniel, S., Joseph, G. M. (2014). Unsteady MHD Couette flow between two infinite parallel porous plates in an inclined magnetic field with heat transfer. *International Journal of Mathematics and Statistics Invention*, 2(3), 103-110.

Kane, I., Kinyanjui, M., & Theuri, D. (2020). Unsteady Fluid Flow Between Two Moving Parallel Porous Plates in the presence of an Inclined Applied Magnetic Field. *Journal of Applied Mathematics and Bioinformatics*, *10*(1), 31-49.

Khan, M. R., Mao, S., Deebani, W., & Elsiddieg, A. M. (2022). Numerical analysis of heat transfer and friction drag relating to the effect of Joule heating, viscous dissipation

and heat generation/absorption in aligned MHD slip flow of a nanofluid. *International Communications in Heat and Mass Transfer*, *131*, 105843.

Kiema, D. W., Manyonge, W. A., Bitok, J. K., Adenyah, R. K., & Barasa, J. S. (2015). On the Steady MHD Couette Flow Between Two Infinite Parallel Plates In a Uniform Transverse Magnetic Field. *J. Appl. Math. Bioinf*, *5*(1), 87-99.

Krishna, M. V. (2016). Unsteady MHD Flow in a Rotating Parallel Plate Channel under the Influence of Pressure Gradient with Hall Current Effects. *Journal of Scientific Research and Reports*, *10*(3), 1-21. https://doi.org/10.9734/JSRR/2016/24123

Malia, M. (2018). Determination of the effect of Applying Variable Pressure Gradient to a Magnetohydrodynamic Fluid flowing between Plates with an Inclined Magnetic Field. *Kenyatta University. November*.

Manyonge, W. A., Kiema, D. W., & Iyaya, C. C. W. (2012). Steady MHD poiseuille flow between two infinite parallel porous plates in an inclined magnetic field. *International journal of pure and applied mathematics*, *76*(5), 661-668.

Mbugua, Z. M., Kinyanjui, M. N., Giterere, K., Kiogora , P. R. (2016). Hydromagnetic fluid between porous parallel plates in the presence of variable transverse magnetic field. *International Journal of Engineering Science and Innovative Technology*, 4(5), 14-22.

Mburu, A., Kwanza, J., & Onyango, T. (2016). Magnetohydrodynamic fluid flow between two parallel infinite plates subjected to an inclined magnetic field under a pressure gradient. *Journal of Multidisciplinary Engineering Sciences & Technology (JMEST)*, *3*(11), 5910-5914.

Moses, J. K., Zakari, T. N., Ibrahim, M. B., & Usman, M. A. (2021). Unsteady MHD Poiseuille Oscillatory Flow between Two Infinite Parallel Porous Plates in an Inclined Magnetic Field with Suction Effect. *KASU Journal of Mathematical Science*, *2*(1), 36-52.

Rajput, U. S., Sahu, P. K. (2011). Transient free convection MHD flow between two long vertical parallel plates with constant temperature variables mass diffusion. *International Journal of Mathematics Analysis*, 34(5), 1665-1671.

Shercliff, J. A. (1953, January). Steady motion of conducting fluids in pipes under transverse magnetic fields. In *Mathematical Proceedings of the Cambridge Philosophical Society* (Vol. 49, No. 1, pp. 136-144). Cambridge University Press.

Singh, C. B. (2014). Hydromagnetic steady flow of liquid between two parallel infinite plates under applied pressure gradient, when upper plate is moving with constant velocity under the influence of inclined magnetic field. *Kenya Journal of Sciences Series A*, *15*(2), 2.

Turkyilmazoglu, M. (2021). Heat transport in shear-driven flow with axial conduction. *Journal of the Taiwan Institute of Chemical Engineers*, *123*, 96-103.

Yasmeen, S., Asghar, S., Anjum, H. J., & Ehsan, T. (2019). Analysis of Hartmann boundary layer peristaltic flow of Jeffrey fluid: Quantitative and qualitative approaches. *Communications in Nonlinear Science and Numerical Simulation, 76,* 51-65.

Zhang, L., Bhatti, M. M., Bég, O. A., Leonard, H. J., & Kuharat, S. (2022). Numerical study of natural convection dissipative electromagnetic non- Newtonian flow through a non- Darcy channel. *ZAMM - Journal of Applied Mathematics and Mechanics/Zeitschrift für Angewandte Mathematik und Mechanik,* e202100608.

APPENDICES

APPENDIX I: MATLAB CODE

```
clear
clc
Pr=0.06;
Ec=0.03;
Pg=-200;
s=450;
Ha=1.1;
M=9.5;
Re=1.25;
tmin=0;
tmax=1.00;
Ny=244;
Ly=246;
%surrounding temperature
tupper=20;tlower=20;tright=20;tleft=20;uupper=20;ulower=20;uleft=20;uri
ght=20;
%initial function
T=zeros(Ny,Ny);
U=zeros(Ny,Ny);
%increment values
dy=Ly/(Ny-1);
delY=dy;
y=0:dy:Ny;
dt=(tmax-tmin)/(Ny-1);
%Initial conditions/
T(1,:)=tupper;
T(Ny,:)=tlower;
T(:,1)=tright;
T(:,Ny)=tleft;
U(1,:)=uupper;
U(Ny,:)=ulower;
U(:,1)=uleft;
U(:,Ny)=uright;
%exterior nodes
for t=tmin:dt:tmax
%interior nodes
for j=2:Ny-1
    for k=1:Ny-1
       U(k,j)=0;
        T(k,j)=0;
    end
end
%porous plate
for j=Ny
   for k=1:Ny
       U(k,j)=-1;
       T(k,j)=0;
   end
end
for j=2:Ny-1
    for k=1:Ny-1
```

```
        %U(K+1,J)=(-Pg-(U(K,J)*s-U(K+1,J-1)-U(K,J-
1))/(2*delY)+(1/Re)*(U(K+1,J+1)+U(K+1,J-1)+U(K,J+1)-2*U(K,J)+U(K,J-
1))/(2*delY*delY))-M*U(K,J))/((s/2*delY)+(1/Re*delY*delY));
        U(k+1,j)=(-Pg-(U(k,j)*s-U(k+1,j-1)-U(k,j-
1))*(2*delY)'+(1/Re)*(U(k+1,j+1)+U(k+1,j-1)+U(k,j+1)-2*U(k,j)+U(k,j-
1))*(2*delY*delY)'-M*U(k,j))/(s*(2*delY)'+(Re*delY*delY)');
        %T(K+1,J)=(-s*(T(K,J)-T(K+1,J-1)-T(K,J-
1))/(2*delY)+0.5/(Pr*delY*delY*Re)*(T(K+1,J-1)+T(K+1,J+1)+T(K,J-
1)2*T(K,J)+T(K,J+1))+(0.5*Ec*(1/Re)*(1/delY*delY))*(U( K+1,J-1)-
2*U(K+1,J)+U(K+1,J-1)-U(K,J-1)-2*U(K,J)+U(K,J-
1))+(Ec*Ha*Ha*U(K,J)*U(K,J))/Re)/((s/(2*delY))+1/(Pr*Re*delY*delY));
        T(k+1,j)=((-s*(T(k,j)-T(k+1,j-1)-T(k,j-
1))/(2*delY)+0.5/(Pr*delY*delY*Re)*(T(k+1,j-1)+T(k+1,j+1)+T(k,j-1)-
2*T(k,j)+T(k,j+1))+(0.5*Ec*(1/Re)*(1/delY*delY))*(U( k+1,j-1)-
2*U(k+1,j)+U(k+1,j-1)-U(k,j-1)-2*U(k,j)+U(k,j-
1))+(Ec*Ha*Ha*U(k,j)*U(k,j))/Re))/(s/(2*delY)+1/(Pr*Re*delY*delY));
    end
end
end
figure(1)
subplot(2,3,1)
v1=plot(U(10,:),'r','Linewidth',1);
title('EFFECTS OF REYNOLD NUMBER ON VELOCITY PROFILES');
xlabel('DISTANCE ');
ylabel('VELOCITY U');
legend('Re=1.25','r')
hold on
v2=plot(U(10,:),'k','Linewidth',1);
hold on
v3=plot(U(10,:),'b','Linewidth',1);
legend([v1,v2,v3],'Re=1.25')
grid off
figure(2)
subplot(2,3,1)
T1=plot(T(10,:),'r','Linewidth',1);
title('EFFECTS OF REYNOLDS NUMBER ON TEMPERATURE PROFILES');
xlabel('DISTANCE');
ylabel('TEMPERATURE T');
hold on
T2=plot(T(10,:),'k','Linewidth',1);
hold on
T3=plot(T(10,:),'b','Linewidth',1);
legend([T1,T2,T3],'Re=1.25');
grid off
```

APPENDIX II: PUBLICATION

Priscilla Twili Kimanthi., Isaac Chepkwony "Effects of Variable Pressure Gradient on Magnetohydrodynamic Flow between Parallel Plates considering Variable Transverse Magnetic Fields" International Journal of Research and Innovation in Applied Science (IJRIAS) volume-7-issue-1, pp.34-39 January 2022 URL: https://www.rsisinternational.org/journals/ijrias/DigitalLibrary/volume-7-issue-1/34-39.pdf